# Effects of quantum fluctuations of electrons and lattice in doped polyacetylene

Akira Takahashi
*Department of Physics, Faculty of Liberal Arts, Yamaguchi University, Yamaguchi 753, Japan*
(Received 18 January 1996; revised manuscript received 6 June 1996)

The effects of quantum fluctuations of electrons and the lattice on the electronic and lattice structures of doped polyacetylene are studied using the quantum Monte Carlo method. We adopt the model where the on-site ($U$) and the nearest-neighbor ($V$) Coulomb interaction terms are added to the Su-Schrieffer-Heeger (SSH) model. In the SSH model, a charged soliton lattice survives quantum fluctuations of the lattice even in the heavily doped regime. However, the magnitude of bond-length alternation in the interface regions between charged solitons is reduced by them. In the model where $U>0$ and $V=0$, the ground state becomes a charged soliton lattice in the low doping regime by introducing quantum fluctuations of electrons. The magnitude of the bond-length alternation in the interface regions decreases with increasing doping concentration and becomes almost zero in the heavily doped regime. In the model where $U>0$ and $V>0$, a charged soliton lattice survives quantum fluctuations of electrons and the lattice even in the heavily doped regime. However, both the magnitude of the bond-length alternation in the interface regions and the magnitude of the charge-density alternation around the soliton centers are reduced by them. The interaction between charged solitons is significantly weakened by quantum fluctuations of electrons, which results in a significant reduction of the charged soliton formation energy in the heavily doped regime. [S0163-1829(96)08535-9]

## I. INTRODUCTION

The Pauli susceptibility rises sharply when the doping concentration ($y$) increases beyond a critical concentration (about 6%).[1,2] This shows that the heavily doped polyacetylene has a finite density of states (DOS) at the Fermi energy. This is confirmed by the transport measurement; the electrical conductivity remains finite as low as 1 mK in some highly conductive samples.[3–5] On the other hand, infrared active vibrational modes, which are ascribed to charged solitons in the low doping regime, persist into the heavily doped regime.[6] This suggests that the ground state in this regime is not the usual metal with a uniform bond length, but a charged soliton lattice.

In simple independent-electron models for a single polyacetylene chain, the ground state is also a charged soliton lattice in the heavily doped regime, and the charged soliton lattice solution has a finite gap at the Fermi energy.[7] Thus the simple model is inconsistent with the experiment. Several theories have been proposed to explain this metallic phase by adding some interactions neglected in the simple model such as effect of disorder,[8–11] interaction with dopant ions,[12,13] and interchain coupling,[14–17] and some of them have succeeded in explaining the metallic phase.

In all the theories mentioned above, quantum fluctuations of both electrons and the lattice have been neglected. However, as shown by Su[18] and others,[19,20] the magnitude of quantum fluctuations of the lattice is almost the same as that of bond-length alternation. Such large fluctuations have been shown to play important roles in the physics of polyacetylene.[20–25] As for the quantum fluctuations of electrons, it is well known that they are very large in one-dimensional systems like polyacetylene and their importance has been confirmed by several studies in short polyenes.[26,27] Thus theories which neglect these two quantum fluctuations or deal with them as small perturbations are not valid in the present case.

Recently, extensive studies have been done on strongly correlated systems away from half-filling, and various interesting physics have been found.[28] However, the present system includes unique physics which, to our knowledge, has not been revealed by these works. First, electron-phonon coupling is essential in the present system. For example, an injected electron or hole accompanies lattice deformation, and results in the formation of a charged soliton or a polaron. Second, most studies have been done in the strongly interacting limit, and charge degrees of freedom have been neglected. However, such an approach is not valid for the present problem because the strength of the Coulomb interaction is in the intermediate regime in polyacetylene. In particular, charge degrees of freedom are important away from half-filling because a charged soliton, which plays important roles there, has a charge-density-wave (CDW)-like electronic structure around the soliton center.[29] Third, only the on-site Coulomb interaction has been considered in most theories. However, the nearest-neighbor interaction is essential to study the electronic structure, particularly away from half-filling, because the CDW-like electronic structure in a charged soliton is stabilized by the nearest-neighbor interaction.[29]

The effects of quantum fluctuations of the lattice in the nearly half-filled Su-Schrieffer-Heeger (SSH) model have been investigated by the author using the adiabatic quantum Monte Carlo (QMC) method.[20] It is shown that quantum fluctuations of the lattice produce a DOS inside the classical gap, and that the gap may be closed in the heavily doped regime. Galli has studied the same problem by the QMC method without the adiabatic approximation, and found that a finite DOS at the Fermi energy is produced by quantum fluctuations of the lattice in the heavily doped regime.[30] However, since his way of calculating the DOS is based on

 

the adiabatic picture, we think the problem is still open. As for the quantum fluctuations of electrons, Takahashi, Yamamoto, and Fukutome have taken account of superpolaron fluctuations in a charged soliton lattice, and have succeeded in showing that metallic properties appear in the heavily doped regime in the extended Hubbard model.[31] However, it is not clear whether this assumption is valid or not. Moreover, since they used the lattice geometry of the Hartree-Fock (HF) charged soliton lattice solution, neither the lattice distortions caused by superpolarons nor quantum fluctuations of the lattice were considered there. Jeckelmann and Baeriswyl showed that the gap is closed in the heavily doped regime in the model where only the on-site Coulomb interaction is considered.[32] However, the nearest-neighbor interaction is important in the present problem, as mentioned above. Moreover, they assumed, that the geometry for equally spaced solitons and geometry optimization has not been done. Quantum fluctuations of the lattice were also not considered in the theory.

Considering the points mentioned before, we investigate the effects of quantum fluctuations of electrons and the lattice away from half-filling in this paper. We adopted the QMC method developed by Hirsch *et al.*[33] This method gives exact electronic and lattice structures of the ground state except for the statistical errors. Thus large and nonlinear fluctuations can be described, and quantum fluctuations of both electrons and the lattice can be taken into account simultaneously by the method. Moreover, the method is applicable to the model which includes not only the on-site Coulomb interaction but also the Coulomb interaction between different sites.

## II. MODEL

As mentioned in Sec. I, both electron-electron and electron-phonon interactions play important roles in polyacetylene. Furthermore, not only the on-site but also the nearest-neighbor Coulomb interactions are important there. Considering these points, we have adopted the following Hamiltonian for a single chain of polyacetylene:

$$H=-\sum_{i,s}\{t_0+\alpha(u_i-u_{i+1})\}\{c^{\dagger}_{i+1,s}c_{i,s}+c^{\dagger}_{i,s}c_{i+1,s}\}+\frac{K}{2}\sum_i (u_{i+1}-u_i-\overline{y})^2+\frac{1}{2M}\sum_i p_i^2+\sum_i \{Un_{i,\uparrow}n_{i,\downarrow}+Vn_in_{i+1}\}. \quad (1)$$

The first three terms show the SSH Hamiltonian, where $u_i$ is the displacement operator of the $i$th CH group along the chain direction, the operator $c_{i,s}$ ($c^{\dagger}_{i,s}$) annihilates (creates) a $\pi$ electron of spin $s$ at the $i$th site, $t_0$ is the mean transfer integral between neighboring electrons, $\alpha$ is the electron-phonon coupling constant, $K$ is the $\sigma$-bond spring constant, $\overline{y}$ is a constant which determines the mean bond length, $M$ is the mass of the CH group, and $p_i$ is the momentum operator conjugate to $u_i$. The fourth term describes the on-site and nearest-neighbor Coulomb interactions between $\pi$ electrons, where $U$ and $V$ are the on-site and the nearest-neighbor repulsions, respectively, and $n_{i,s}$ is the electron-density operator of spin $s$ at the $i$th site given by

$$n_{i,s}=c^{\dagger}_{i,s}c_{i,s} \quad (2)$$

and

$$n_i=n_{i,\uparrow}+n_{i,\downarrow}. \quad (3)$$

A linear chain is considered in this paper because we need not consider the global flip between QMC samples with different winding numbers in this case.[33]

We considered the following three sets of the parameters which have been shown to be appropriate for polyacetylene by previous works.[6,32,34] In the SSH-extended Hubbard model, $t_0=2.5$ eV, $\alpha=4.07$ eV Å$^{-1}$, $K=42$ eV Å$^{-2}$, $M=3145$ eV$^{-1}$ Å$^{-2}$, $U/t_0=2.5$, and $V/t_0=1.25$. $\overline{y}$ is determined as described in the following to minimize the boundary effects. First, we obtained the geometry optimized half-filled HF solutions both in a periodic chain and in a linear chain. The HF solution is uniformly dimerized, and does not depend on $\overline{y}$ in the periodic chain. On the other hand, the HF solution is almost uniformly dimerized except for the chain edge regions, and it depends on $\overline{y}$ in the linear chain. We chose the value of $\overline{y}$ so that the mean bond length in the uniformly dimerized region in the linear chain is the same as that of the periodic chain; $\overline{y}=0.123$ Å. In the SSH-Hubbard model, $V/t_0=0$ and the other parameters are the same as those in the SSH-extended Hubbard model. In the SSH model, $K=21$eV Å$^{-2}$, $\overline{y}=0.243$ Å, $U/t_0=V/t_0=0$, and the other parameters are the same as those in the two models.

The expectation values of various physical quantities were obtained by the QMC method. The inverse of the temperature $\beta$ was taken to be 40 eV$^{-1}$. Since $\beta\omega_0=4$, where $\omega_0=\sqrt{4K/M}$ is the bare optical-phonon frequency, the effects of thermal phonon excitations can be neglected. The Trotter number for electrons and that for phonons were taken to be 1200 and 40, respectively, in models including the Coulomb interaction, and they were taken to be 400 and 10, respectively, in the SSH model. To check the validity of these values, we calculated the ground-state energy when $\alpha=0$ using the periodic boundary condition. In this case, the phonon part of the present Hamiltonian is that of the coupled harmonic oscillators and the electronic part of the present Hamiltonian is Hubbard (Hückel) Hamiltonian when $V=0$ ($U=V=0$). These models can be solved exactly. We compared the energies of these two parts obtained by the present method with those of the exact solutions, and found that the errors in them were both within a few percent.

To compare with QMC results, we also obtained the same physical quantities by using the classical lattice and HF approximations. In the classical lattice approximation, only lattice degrees of freedom were treated classically by taking the Trotter number for phonons to be 1 in the QMC simulation. In the HF approximation, the lattice coordinates were treated classically and the electronic and lattice structures were self-consistently determined so as to satisfy Hellmann-Feynman force equilibrium.

For the convenience in the following, we here introduce two important physical quantities: the charge density (CD) and the lattice order parameter (LOP). The electronic and

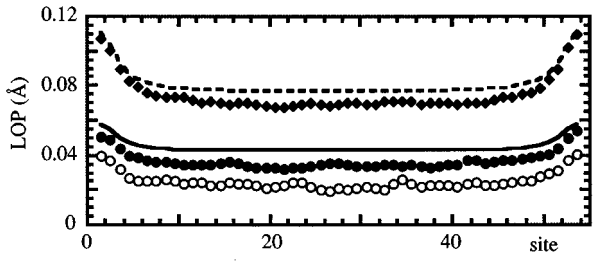


FIG. 1. The LOP distribution of the ground state in the half-filled case. In the SSH model, that obtained by the classical lattice approximation is shown by the broken line, and that obtained by the QMC method is shown by the closed diamonds. In the SSH-extended Hubbard model, that obtained by the HF approximation is shown by the solid line and that obtained by the QMC method is shown by the closed circles. In the SSH-Hubbard model, that obtained by the QMC method is shown by the open circles.

lattice structures of a charged soliton are characterized by them. The CD at the $i$th site is given by

$$d_i = 1 - \sum_s \langle c_{i,s}^\dagger c_{i,s} \rangle, \tag{4}$$

where $\langle O \rangle$ indicates the expectation value of an operator $O$. The deviation of the bond length from the mean bond length at the $i$th bond is given by

$$y_i = \langle u_{i+1} \rangle - \langle u_i \rangle. \tag{5}$$

These quantities are decomposed into nonalternating and alternating components as

$$d_i = \overline{d_i} + (-1)^i d_i' ,$$

$$y_i = \overline{y_i} + (-1)^i y_i' , \tag{6}$$

where nonalternating and alternating components are represented by the bar and prime, respectively. The operational definition of $d_i$ is

$$\overline{d_i} = \tfrac{1}{4}(d_{i-1} + 2d_i + d_{i+1}), \tag{7}$$

and the same formulae can be used for $\overline{y_i}$.[35] The LOP at the $i$th bond is defined by $y_i'$ namely, the alternating component of the deviation of the bond length. Hence the LOP shows the strength of the bond-length alternation, including the phase of the alternation. A bond order wave (BOW) state, where the bond length alternates uniformly, is characterized by a uniform and finite LOP, and a CDW state is also characterized by a uniform and finite $d_i'$.

## III. RESULTS AT HALF-FILLING

Before turning to the results away from half-filling, we first discuss the half-filled case. We show the LOP distributions of the half-filled ground states in the three models in Fig. 1. The system size $N$ is taken to be 54. Note that the ground states have no CD in all the models.

### A. SSH model

In the SSH model, the LOP is finite and almost uniform except for the chain edge regions, and the ground state is a BOW state within the classical lattice approximation. The LOP becomes larger near the chain ends because of a boundary effect.

The bond-length alternation survives quantum fluctuations of the lattice, but the magnitude of the LOP is reduced by them. We define the average magnitude of the LOP by

$$\overline{y'} = \frac{1}{N-15} \sum_{i=8}^{N-8} y_i' . \tag{8}$$

To reduce the boundary effect, the LOP's at the seven bonds from each chain edge were excluded from the average. The average magnitude $\overline{y'}$ is reduced by 9% by introducing quantum fluctuations of the lattice. This value is consistent with that obtained by the adiabatic QMC method.[20] This is an expected result because the energy gap is much larger than $\omega_0$, and the adiabatic approximation is good in this case. However, this value is smaller than those obtained in earlier works.[18,19] We think that this is because much smaller systems were considered there.

### B. SSH-Hubbard model

Within the HF approximation, $U$ stabilizes a spin-density wave (SDW) state, but the HF energy of a BOW state is independent of $U$.[36] As a result, the HF ground state is a SDW state in this model with the present parameters.

Next, we consider the effects of quantum fluctuations. In this SSH-Hubbard model and also in the SSH-extended Hubbard model, the LOP distribution obtained by the classical lattice approximation is almost the same as that obtained by the QMC method, in contrast to the SSH model. Thus the effects of quantum fluctuations of the lattice on the LOP are very small in these two models, including the Coulomb interaction.

When quantum fluctuations of electrons are taken into account, a finite LOP appears, as seen from Fig. 1, and a BOW state becomes the ground state in this model. This is because the correlation energy of a BOW state is larger than that of a SDW state. This result is consistent with previous ones.[37–40]

### C. SSH-extended Hubbard model

Within the HF approximation, a BOW state is stabilized by $V$,[36] and the HF ground state again becomes a BOW state as seen from Fig. 1. Thus $U$ and $V$ have opposite effects on the LOP within the HF approximation.

The bond-length alternation survives quantum fluctuations of electrons, but they reduce $\overline{y'}$ by 19% in this model. Thus correlations by $U$ and $V$ have also the opposite effects on the LOP.

## IV. RESULTS AWAY FROM HALF-FILLING

We now consider the case away from half-filling. The following three different doping concentrations were considered : $y=4\%$ ($\nu=2$ and $N=50$, where $\nu$ is the net charge), $y=7.7\%$ ($\nu=4$ and $N=52$), and $y=11\%$ ($\nu=6$ and

$N=54$). The doping concentration $y=4\%$ belongs to the nonmagnetic regime. The other ones belong to the metallic regime, and $y=7.7\%$ is just above the critical doping concentration when the experimentally observed metal-insulator transition occurs. There are two kinds of charged solitons with different interface structures.[35] In order to set all the charged solitons to be of one kind, we could not fix $N$. We show the LOP, CD, nonalternating CD and alternating CD distributions of the ground state at 11% doping in the SSH model in Fig. 2(a), and those in the SSH-extended Hubbard and the SSH-Hubbard models in Fig. 2(b).

As seen from Fig. 2, the distribution of the nonalternating CD is almost independent of the models and approximations considered here. The nonalternating CD decreases near chain edges, where the LOP, and therefore the bond-order alternation, becomes large. This is because the strong bond-order alternation is incompatible with a large CD.[36]

Conversely, the alternating CD and LOP distributions depend strongly on the models and approximations. To do a more quantitative study, we define the amplitude of oscillating $y_i'$ and $d_i'$ of a charged soliton lattice in the following way. In the continuum version of the Pariser-Par-Pople model, the analytic HF solution of a charged soliton lattice has been obtained.[41] In the solution, $y_i'$ and $d_i'$ in the heavily doped regime are given by

$$y_i' = \tilde{y}' \cos\left(\frac{\pi n_s i}{N}\right), \tag{9}$$

$$d_i' = \tilde{d}' \sin\left(\frac{\pi n_s i}{N}\right), \tag{10}$$

where $n_s$ is the number of charged solitons. The amplitudes $\tilde{y}'$ and $\tilde{d}'$ are obtained by fitting these curves to the data using the least-squares method. To eliminate the boundary effects, the data at seven sites or seven bonds from each chain edge are not used. The distributions of $y_i'$ and $d_i'$ could be nicely fitted by these curves at 7.7% and 11% doping. We show the $y$ dependences of $\tilde{y}'$ and $\tilde{d}'$ in Fig. 3. We plot $\overline{y'}$ as $\tilde{y}'$ at $y=0$.

### A. SSH model

As seen from Fig. 2(a), the ground state of this model within the classical lattice approximation has electronic and lattice structures characteristic of a charged soliton lattice; the sign of the LOP is reversed at the soliton centers, and a CDW-like structure appears around the soliton centers.

In the QMC method, a long sequence of classical lattice configurations (QMC samples) are generated. Each configuration appears in the sequence with a probability proportional to its probability distribution in the quantum ground state. We show the LOP distributions of three randomly picked up QMC samples in Fig. 4. As seen from the figure, the magnitude of quantum fluctuations of the lattice is larger than $\tilde{y}'$. The result is consistent with previous ones at half-filling.[9,20] As seen from Figs. 2(a) and 3, however, $\tilde{y}'$ remains finite when quantum fluctuations of the lattice are introduced, and the characteristic structures of a charged soliton lattice survive them even at the heaviest doping concentration considered here. The result can be understood as follows. As shown by previous works,[9,20] each lattice site fluctuates almost independently. As a result, contributions of the collective tunneling fluctuations between two degenerate

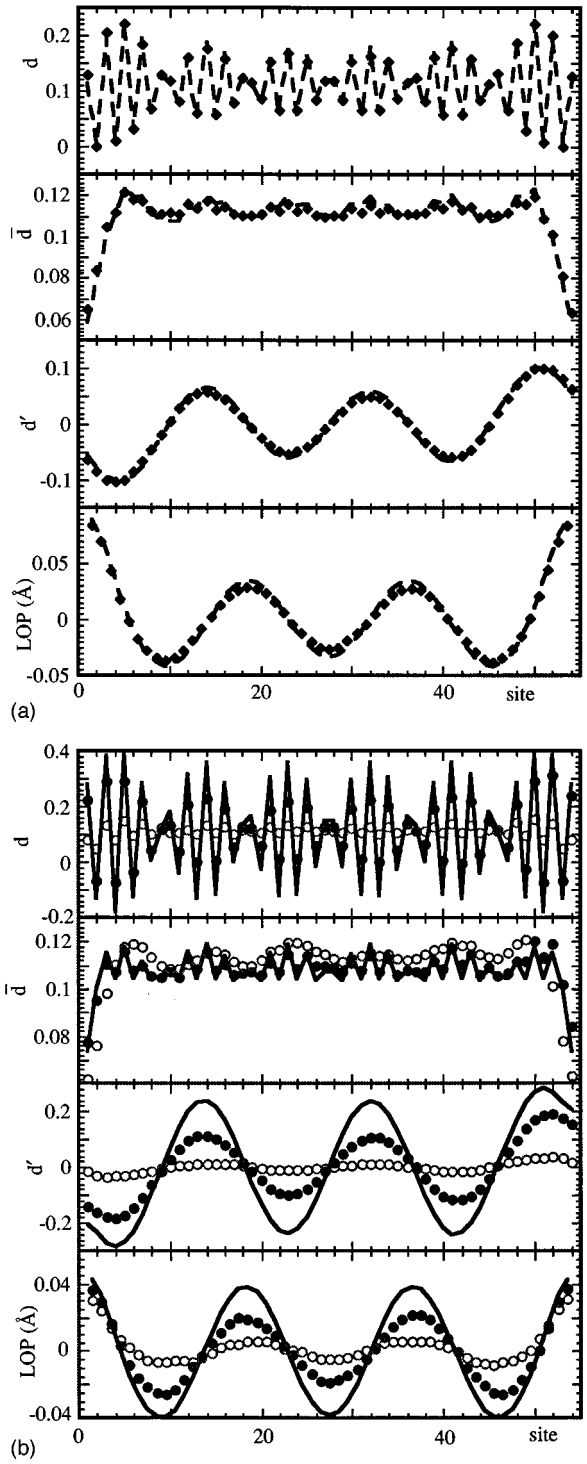


FIG. 2. The LOP, CD, nonalternating CD and alternating CD distributions of the ground state in the case of 11% doping. (a) In the SSH model, those obtained by the classical lattice approximation are shown by the broken lines, and those obtained by the QMC method are shown by the closed diamonds. (b) In the SSH-extended Hubbard model, those obtained by the HF approximation are shown by the solid lines, and those obtained by the QMC method are shown by the closed circles. In the SSH-Hubbard model, those obtained by the QMC method are shown by the open circles.

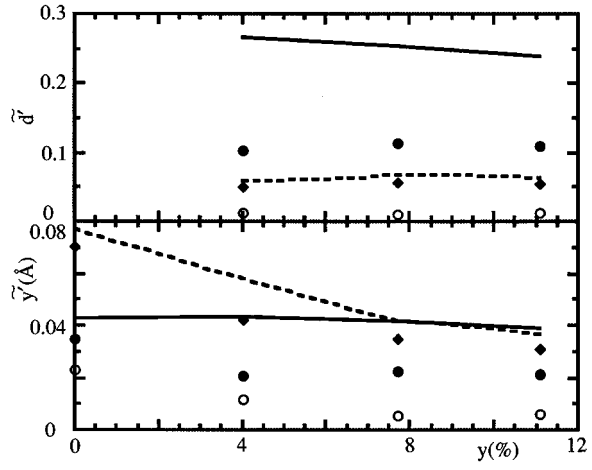


FIG. 3. The $y$ dependences of $\tilde{y}'$ and $\tilde{d}'$. In the SSH model, those obtained by the classical lattice approximation are shown by the broken lines, and those obtained by the QMC method are shown by the closed diamonds. In the SSH-extended Hubbard model, those obtained by the HF approximation are shown by the solid lines, and those obtained by the QMC method are shown by the closed circles. In the SSH-Hubbard model, those obtained by the QMC method are shown by the open circles.

phases of bond-length alternation, which destroy the finite LOP, are negligible in this case.

The amplitude $\tilde{y}'$ is reduced by quantum fluctuations of the lattice. The reduction in $\tilde{y}'$ is the largest (25%) at $y=4\%$. The large reduction can be attributed to the fluctuation of the positions of the charged solitons for the following reasons. First, the fluctuation reduces $\tilde{y}'$ on average. Moreover the fluctuation is much larger at $y=4\%$ than at $y=7.7\%$ or 11% because the interaction between adjacent charged solitons is much weaker there. Second, the fluctuation can be seen directly. We divided the QMC samples into several blocks. By comparing averaged CD and LOP distributions for each block, we can see that the positions of the charged solitons fluctuate very slowly when $y=4\%$.

In the heavily doped regime, the reductions in $\tilde{y}'$ by quantum fluctuations of the lattice (16% at $y=11\%$ and 17% at $y=7.7\%$) are still larger than that of the half-filled case. This can be interpreted as follows. As $y$ increases, the ratio of the BOW region, where the LOP is finite, decreases, and the adiabatic potential as a function of $\tilde{y}'$ becomes shallower. As a result, the effects of noncollective fluctuations, where each site fluctuates almost independently, are enhanced in the heavily doped regime.

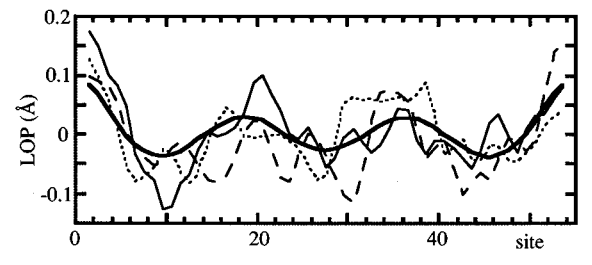


FIG. 4. The LOP distributions of the randomly picked up three QMC samples in the SSH model in the case of 11% doping, are shown by the thin solid, broken, and dotted lines. The LOP distribution (expectation value) of the ground state obtained by the QMC method is shown by the thick solid line.

### B. SSH-Hubbard model

By introducing $U$, the HF ground state becomes a SDW state at half-filling, as mentioned above. As a result, the HF charged soliton lattice solution is unstable in this model.

We next consider the effects of quantum fluctuations. In the same way as in Sec. IV A, we can see that the magnitude of the quantum fluctuations of the lattice is very large in this SSH-Hubbard model, and also in the SSH-extended Hubbard model. However, the LOP and CD distributions obtained by the classical lattice approximation and those obtained by the QMC method are almost the same away from half-filling in these two models. Thus, the effects of quantum fluctuations of the lattice on these expectation values are very small in these two models including the Coulomb interaction.

When quantum fluctuations of electrons are introduced, finite $\tilde{y}'$ appears as seen from Fig. 3, and the ground state becomes a charged soliton lattice at $y=4\%$. This comes from the stabilization of a BOW state by them. However, $\tilde{y}'$ decreases with increasing $y$, and the bond lengths become almost uniform in the heavily doped regime as seen from Fig. 3. The result is consistent with that obtained by Jeckelmann and Baeriswyl,[32] except that $\tilde{y}'$ at $y=4\%$ is much smaller in the present case. In their calculation, lattice structure of equally spaced solitons is assumed, and the fluctuation of the positions of the charged solitons mentioned before is not considered. We think that the difference can be attributed to this point.

In this model, $\tilde{d}'$ is almost zero at all doping concentrations considered in this paper, as seen from Fig. 3. This is because the HF energy is increased by CD alternation in this model.[36]

### C. SSH-extended Hubbard model

First, we consider the effects of the Coulomb interaction within the HF approximation. Since a BOW state is stabilized by $V$, the HF ground state again becomes a charged soliton lattice in this model, as seen from Fig. 2(b). As seen from Fig. 3, $\tilde{d}'$ in this model is much larger than that in the SSH model in spite of the fact that the distributions of nonalternating CD are almost the same in these models. This is because the CDW-like electronic structure is stabilized by $V$. The amplitude $\tilde{y}'$ decreases with increasing $y$ in the SSH model, while $\tilde{y}'$ is almost constant to $y$ in this model. This comes from the fact that a soliton is an amplitude soliton in the SSH model, but is a phase soliton in this model.[41]

When quantum fluctuations of electrons are introduced, $\tilde{y}'$ and $\tilde{d}'$ remain finite even at the highest doping considered here, as seen from Fig. 3. This indicates that a charged soliton lattice survives them even in the heavily doped regime.

The quantum fluctuations of electrons reduce both $\tilde{y}'$ and $\tilde{d}'$. The reductions both in $\tilde{y}'$ and in $\tilde{d}'$ are nearly independent of $y$ away from half-filling and the reduction in $\tilde{y}'$ is larger away from half-filling than at half-filling. This can be understood in the same way as the SSH model; the

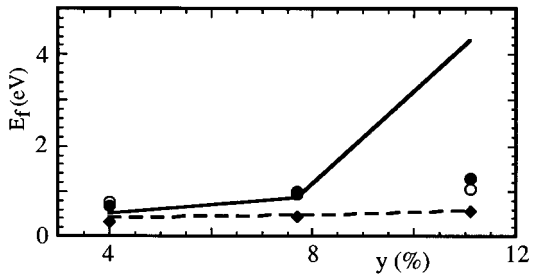


FIG. 5. The $y$ dependences of $E_f$. In the SSH model, that obtained by the classical lattice approximation is shown by the broken line, and that obtained by the QMC method is shown by the closed diamonds. In the SSH-extended Hubbard model, that obtained by the HF approximation is shown by the solid line, and that obtained by the QMC method is shown by the closed circles. In the SSH-Hubbard model, that obtained by the QMC method is shown by the open circles.

fluctuation of the positions of the charged solitons reduces $\tilde{y}'$ in the low doping regime, and noncollective fluctuations, which also reduce $\tilde{y}'$, increase in the heavily doped regime because the HF energy potential becomes shallow there.

### D. Formation energy

The formation energy of a charged soliton $E_f$ is defined by

$$E_f=\{E(+\nu)+E(-\nu)-2E(0)\}/(2\nu), \tag{11}$$

where $E(\pm\nu)$ is the ground-state energy when the net charge is $\pm\nu$, and $E(0)$ is that of the half-filled case. Using the anion-cation symmetry of the present Hamiltonian, we obtain

$$E_f=\{E(+\nu)-E(0)+U\nu/2\}/\nu. \tag{12}$$

We show the $y$ dependence of $E_f$ in Fig. 5.

In the SSH model, $E_f$ increases slightly with increasing $y$, and the effects of quantum fluctuations of the lattice on $E_f$ are small. Conversely, in the SSH-extended Hubbard model, $E_f$ obtained by the HF approximation increases rapidly in the regime $y>8\%$, where the adjacent charged solitons strongly overlap. This indicates that the interaction between them is very strong in this regime in this case, and that the increase in $E_f$ can be attributed to the soliton-soliton interaction energy. By introducing quantum fluctuations of electrons, $E_f$ is slightly increased at $y=4\%$ and 7.7%. The small increase in the regime where the soliton-soliton interaction energy is small can be attributed to the increase in the formation energy of an isolated charged soliton. This shows that stabilization by quantum fluctuations in the BOW phase is larger than that in the CDW phase around the charged soliton centers. On the other hand, $E_f$ is significantly reduced by quantum fluctuations of electrons at $y=11\%$. The large reduction implies that the interaction between adjacent charged solitons is weakened significantly by them. This is partially because the magnitudes of both bond-length and CD alternations are reduced by them.

## V. DISCUSSIONS

As shown in Sec. IV, $\tilde{y}'$ becomes almost zero in the heavily doped regime in the SSH-Hubbard model. Jeckelmann and Baeriswyl obtained a similar result using the variational approach with the Gutzwiller wave function.[32] They further showed that the energy gap also becomes almost zero in the regime as a result of the vanishing LOP. Thus they proposed that the metal-insulator transition can be explained in the SSH-Hubbard model. As shown in Sec. IV, however, $V$ has effects on the electronic and lattice structures which cannot be described by $U$, and a finite LOP survives even in the heavily doped regime in the SSH-extended Hubbard model. Since it is not natural to assume that only $V$ is strongly screened in polyacetylene, we conclude that quantum fluctuations of electrons reduce the energy gap, but that it remains finite even in the heavily doped regime; the metal-insulator transition can not be explained by a simple single-chain model.

We have not considered some important effects such as interchain coupling, the electric field from dopant ions, and disorder. It will be necessary to consider them to explain the metal-insulator transition in polyacetylene. Among them, the last two effects can be taken into account straightforwardly by the present method. The electric field from dopant ions pins charged solitons, and strongly suppresses the fluctuation of their positions. As a result, it probably reduces the correlation effects on the electronic and lattice structures of a charged soliton lattice in the lightly doped regime. As for the effects of disorder, since the interaction between charged solitons is significantly weakened by quantum fluctuations of electrons, the electric field from disordered dopant ions, for example, causes stronger effects on the arrangement of charged solitons when quantum fluctuations are considered. In this way, these two effects which are not considered in this paper, couple with the effects of quantum fluctuations. These are subjects of a future study.

It is widely accepted that charged solitons carry electronic current in the nonmagnetic regime.[6] However, the conduction mechanism remains to be explained as noted from the beginning of the soliton model.[42] The problem is that charged solitons are pinned by the electric field from dopant ions, and the pinning potential (about 0.1 eV) is too strong to be unpinned by the thermal fluctuations. To explain the unpinning mechanism, Fukutome and Takahashi proposed a conduction mechanism in which electronic current is carried by interstitial solitons and soliton holes in a pinned charged soliton lattice produced by thermal excitations.[43] The theory has been improved by several authors.[44,45] The formation and pinning energies of these defects were calculated using the HF approximation in these papers. However, because of the strong interaction between charged solitons, these energies are too large to explain the high conductivity in this regime. Since the interaction is significantly weakened by introducing quantum fluctuations of electrons, the unpinning mechanism may be explained by the theory when fluctuations are taken into account. In this way, quantum fluctuations may also play an important role in the conduction mechanism in this regime.

[1] J. Chen, T. -C. Chung, F. Moraes, and A. J. Heeger, Solid State Commun. **53**, 757 (1985).
[2] F. Moraes, J. Chen, T.-C. Chung, and A. J. Heeger, Synth. Met. **11**, 271 (1985).
[3] Y. Nogami, H. Kaneko, H. Itoh, T. Ishiguro, T. Sasaki, N. Toyota, A. Takahashi, and J. Tsukamoto, Phys. Rev. B **43** 11 829 (1991).
[4] T. Ishiguro, H. Kaneko, Y. Nogami, H. Ishimoto, H. Nishiyama, J. Tsukamoto, A. Takahashi, M. Yamamura, T. Hagiwara, and K. Sato, Phys. Rev. Lett. **69**, 660 (1992).
[5] T. Ishiguro, H. Kaneko, J. P. Pouget, and J. Tsukamoto, Synth. Met. **69**, 37 (1995).
[6] A. J. Heeger, S. Kivelson, J. R. Schrieffer, and W.-P. Su, Rev. Mod. Phys. **60**, 781 (1988), and references therein.
[7] A. Takahashi, Prog. Theor. Phys. **81**, 610 (1989).
[8] E. J. Mele and M. J. Rice, Phys. Rev. B **23**, 5387 (1981).
[9] W. P. Su, Solid State Commun. **47**, 947 (1983).
[10] K. Harigaya and A. Terai, Phys. Rev. B **44**, 7835 (1991).
[11] S. Stafström, Phys. Rev. B **43**, 9158 (1991).
[12] E. M. Conwell and S. Jaydev, Phys. Rev. Lett. **61**, 361 (1988).
[13] E. M. Conwell, H. A. Mizes, and S. Jaydev, Phys. Rev. B **40**, 1630 (1989).
[14] H. A. Mizes and E. M. Conwell, Phys. Rev. B **43**, 9053 (1991).
[15] S. Stafström, Phys. Rev. B **47**, 12 437 (1993).
[16] A. Yamashiro, A. Ikawa, and H. Fukutome, Synth. Met. **65**, 233 (1994).
[17] M. I. Salkola and S. A. Kivelson, Phys. Rev. B **50**, 13 962 (1994).
[18] W. P. Su, Solid State Commun. **42**, 497 (1982).
[19] E. Fradkin and J. E. Hirsch, Phys. Rev. B **27**, 1680 (1983).
[20] A. Takahashi, Phys. Rev. B **46**, 11 550 (1992); Synth. Met. **55-57**, 4485 (1993).
[21] J. Yu, H. Matsuoka, and W. P. Su, Phys. Rev. B **37**, 10 367 (1988).
[22] B. Friedman and W. P. Su, Phys. Rev. B **39**, 5152 (1989).
[23] R. H. McKenzie and J. W. Wilkins, Phys. Rev. Lett. **69**, 1085 (1992).
[24] T. W. Hagler and A. J. Heeger, Chem. Phys. Lett. **189**, 333 (1992); Phys. Rev. B **49**, 7313 (1994).
[25] A. Takahashi, Phys. Rev. B **51**, 16 479 (1995).
[26] K. Schulten, I. Ohmine, and M. Karplus, J. Chem. Phys. **64**, 4422 (1976).
[27] I. Ohmine and M. Karplus, J. Chem. Phys. **68**, 2298 (1978).
[28] See, for example, A. Auerbach, *Interacting Electrons and Quantum Magnetism* (Springer-Verlag, New York, 1994).
[29] H. Fukutome and M. Sasai, Prog. Theor. Phys. **69**, 373 (1983).
[30] L. Galli, Phys. Rev. B **51**, 6863 (1995).
[31] A. Takahashi, S. Yamamoto, and H. Fukutome, J. Phys. Soc. Jpn. **61**, 199 (1992).
[32] E. Jeckelmann and D. Baeriswyl, Synth. Met. **65**, 211 (1994).
[33] J. E. Hirsch, R. L. Sugar, D. J. Scalapino, and R. Blankenbecler, Phys. Rev. B **26**, 5033 (1982).
[34] J. E. Hirsch and M. Grabowski, Phys. Rev. Lett. **52**, 1713 (1984).
[35] A. Takahashi and H. Fukutome, Solid State Commun. **62**, 279 (1987).
[36] H. Fukutome and M. Sasai, Prog. Theor. Phys. **69**, 1 (1983).
[37] P. Horsch, Phys. Rev. B **24**, 7351 (1981).
[38] J. E. Hirsch, Phys. Rev. Lett. **51**, 296 (1983).
[39] D. Baeriswyl and K. Maki, Phys. Rev. B **31**, 6633 (1985).
[40] G. W. Hayden and Z. G. Soos, Phys. Rev. B **38**, 6075 (1988).
[41] M. Sasai and H. Fukutome, Prog. Theor. Phys. **73**, 1 (1985).
[42] W. P. Su, J. R. Schrieffer, and A. J. Heeger, Phys. Rev. B **22**, 2009 (1980).
[43] H. Fukutome and A. Takahashi, Prog. Theor. Phys. **77**, 1376 (1987).
[44] A. Takahashi and H. Fukutome, Synth. Met. **28**, D469 (1989).
[45] A. Yamashiro, A. Ikawa, and H. Fukutome, Prog. Theor. Phys. **113**, 25 (1993).